Journal Pre-proofs

Analysis of the Effects of Ultraviolet and Infrared Lamps on the Physical and Chemical Properties of Eggs Using Principal Component Analysis Method

Mohammad javad Mahmoodi, Mohsen Azadbakht, Behrouz Dastar, Ali Asghari

DOI: https://doi.org/ 10.22104/ift.2025.7875.2238

To appear in: Innovative Food Technologies (IFT)

Received Date: 16 September 2025 Revised Date: 18 October 2025 Accepted Date: 19 October 2025



Please cite this article as: Mohammad javad Mahmoodi, Mohsen Azadbakht, Behrouz Dastar, Ali Asghari, Analysis of the Effects of Ultraviolet and Infrared Lamps on the Physical and Chemical Properties of Eggs Using Principal Component Analysis Method, *Innovative Food Technologies* (2025), doi: https://doi.org/10.22104/ift.2025.7875.2238

This is a PDF file of an article that has undergone enhancements after acceptance, such as the addition of a cover page and metadata, and formatting for readability, but it is not yet the definitive version of record. This version will undergo additional copyediting, typesetting and review before it is published in its final form, but we are providing this version to give early visibility of the article. Please note that, during the production process, errors may be discovered which could affect the content, and all legal disclaimers that apply to the journal pertain.

© 2023 The Author(s). Published by irost.org.

Analysis of the Effects of Ultraviolet and Infrared Lamps on the Physical and Chemical Properties of Eggs Using Principal Component Analysis Method

Mohammad javad Mahmoodi ¹, Mohsen Azadbakht ^{2*}, Behrouz Dastar ³, Ali Asghari ⁴

Tel & Fax: +981732440870 * azadbakht@gau.ac.ir

Abstract

Given the critical importance of egg quality for consumer health and the prevention of economic losses in the industry, identifying factors that help maintain or enhance quality is essential. This study aimed to investigate the effects of the number and exposure time of ultraviolet and infrared lamps on the quality characteristics of eggs using principal component analysis. A total of 56 intact eggs were collected and subjected to pre-treatments with ultraviolet and infrared lamps, both with and without sunflower oil coating. Subsequently, quality parameters of the samples were measured, and the resulting data were evaluated using Principal Component Analysis. The Principal Component Analysis results indicated that the type and intensity of ultraviolet and infrared irradiation had distinct impacts on egg quality attributes. ultraviolet exposure produced more diverse patterns, whereas infrared exposure resulted in more uniform responses. Quality variables such as volume, density, crude protein, and total ash played the most significant roles in differentiating the treatments. Moreover, prolonged exposure time intensified differences between groups, highlighting Principal Component Analysis as an effective tool for identifying key factors influencing egg quality.

Keywords: Egg, Ultraviolet, Physical and Chemical Properties, PCA Method

Introduction

Nowadays, the use of eggs as a complete nutritional package has become increasingly widespread, both directly and indirectly. Therefore, their quality holds significant importance [1]. The concept of quality in eggs is highly complex and encompasses various attributes, including egg size, shell color and integrity, shape, and internal quality characteristics [2]. Immediately after laying, the deterioration process of the egg characterized by chemical and nutritional changes begins, accompanied by the release of CO₂ and alterations in pH levels [3]. Furthermore, the deterioration of egg albumen during storage depends on storage conditions (temperature and relative humidity) as well as the characteristics of the eggshell [4]. The duration of storage is generally used as a key indicator for distinguishing between fresh eggs and

¹ Master's degree graduate in Biosystems Engineering, Gorgan University of Agricultural Sciences and Natural Resources, Gorgan, Iran.

² Professor of Department of Biosystems Engineering, Gorgan University of Agricultural Sciences and Natural Resources, Gorgan, Iran.

³Professor of Department of Animal and Poultry Nutrition, Faculty of Animal Science, Gorgan University of Agricultural Sciences and Natural Resources, Gorgan, Iran.

⁴ Research Professional, Department of Soils and Agri-Food Engineering, Université Laval, Quebec, Canada.

those suitable for consumption [5]. However, considering the points mentioned above, the number of days post-laying alone cannot be relied upon. Therefore, variable chemical indicators during storage are regarded as key determinants of egg freshness [6]. The egg industry worldwide is responsible for producing eggs with high internal and external quality, which is essential for its economic sustainability. Currently, egg quality issues impose significant costs on the industry. So, understanding the factors that influence both internal and external quality is of great importance. In light of these considerations, eggs must be evaluated in terms of both internal and external quality. In the past, various methods have been employed to assess the internal contents of eggs, which can generally be categorized into destructive and nondestructive techniques [7]. One advantage of various destructive methods over non-destructive techniques is that measurements can be performed directly on the internal contents of the egg [8]. However, in this approach, eggs must be broken, which limits testing to a small number of samples. Moreover, destructive evaluation methods are time-consuming and require specialized sample preparation [9]. On the other hand, in non-destructive methods, attributes related to the albumen and yolk are measured in intact eggs. These assessments can be performed on the production line, in real time, and are applicable to all eggs [10]. Cedro et al. (2009) investigated the internal contents of eggs, analyzing the yolk and albumen separately, to examine the effect of storage duration on pH levels. The storage period was set at 44 days. Their results showed that with increasing storage time, the pH of both the yolk and albumen increased significantly [11]. In other studies in this field, the effect of storage time on the protein content of eggs was examined, and researchers concluded that prolonged storage leads to a decrease in egg protein content. In general, the evaluation of physical and chemical characteristics of agricultural products can be reflected by various indicators; however, comprehensive analysis of these dispersed indicators is challenging. Principal Component Analysis (PCA) is an analytical method that summarizes numerous variables into a few comprehensive components and explains the correlations among different variables, along with Pearson correlation analysis [12]. Ultimately, considering the critical importance of egg quality, examining the factors that contribute to its preservation or deterioration during storage is essential. Despite various studies conducted on egg quality assessment, a comprehensive analysis using PCA to evaluate the effects of different influencing factors has not yet been performed. Therefore, the objective of this study is to investigate the effects of the number and exposure time of UV and IR lamps on the qualitative attributes of eggs through principal component analysis.

Materials and methods

Samples preparation and treatment selection

In this study, 56 healthy eggs were collected from an egg layer flock (Hyline W36 strain with 30 weeks of egg) in a private company near the city of Gorgan, Golestan province on October 13, 2018. The eggs produced were prepared with an average weight of 72 g and then transferred to Gorgan University of Agricultural Sciences and Natural Resources.and then transferred to Gorgan University Agricultural Sciences and Natural Resources, Gorgan, Iran. A total of 28 eggs were exposed to UV radiation and also another 28 eggs were subjected to IR radiation, next each group was divided into sunflower oil-smeared and non-smeared categories. The sunflower was used because of its positive effect on shelf life and eggs quality. The samples were stored for two days then the physical and mechanical properties were measured.

Moisture measurement

After the egg contents were placed in an oven at 100°C for 24 h, the moisture content was measured by the weight loss method, according to Azadbakht et al., 2016. The egg contents were dried until a constant weight was achieved, indicating negligible further moisture loss, over a 24-hour period.

Ultraviolet radiation method

As shown in figure 1, the UV light was produced by an array of LEDs. The specifications for these LEDs were as follows: 3mm in diameter, a wavelength of 400 nm (within the UV-A spectrum) and an operating voltage of 3-4 volts. The light source was positioned parallel to the floor at a height of 40 cm above the samples. The entire circuit operated at 12 volts and 0.84 amperes, and the UV radiation was applied over an area of $20 \times 50 \text{ cm}^2$ [14].

Figure 1. Schematic of the circuit and the Ultraviolet radiation method (1) Sample location; (2) lamp circuit; (3) radiation chamber

Infrared radiation method

In figure 2 the source of IR light and the egg radiation method are shown. In this method several IR LEDs are used, the specification of LEDs were 3 mm in diameter, 850 nm in wavelength and 3.3-4 volts in voltage The distance of IR light source and samples was parallel to the floor in height of 40cm. The characteristics of the whole circuit were 12 volts, 0.84 amperes and the area of the use of IR radiation was $50\times20 \text{ cm}^2$ [15].

Figure 2. Schematic of the circuit and the Infrared radiation method (1) Sample location; (2) lamp circuit; (3) radiation chamber

Quasi-static test

The required failure force of eggshells under quasistatic loading was investigated in three cases of impregnated specimens without impurities in sunflower oil under the magnetic field and control. Quasi-static loading indicates sample resistance to failure, so the extracted data is suitable for investigating the effect of the IR and UV radiated and impurity on sunflower oil. For thin edge quasi-static testing was performed using an universal testing machine (Santam-STM5 - SANTAM Engineering and Design Company, Tehran, Iran) device with a load of 500 N strain for the pressure test, the thin edge of a plastic jaw was considered with a surface of 3×15 mm (Figure 3). In order to increase the accuracy of the measurement, the speed of the device when applying the pressure force was 0.33 mm/min, in the direction of the z-axis (Figure 4) and in three replications was performed, and as a result failure force of the eggshell was obtained. The direction of compressive force was chosen in the direction of the z-axis due to the high vulnerability of the egg. Loading was continued until the egg shell's failure, and then the force-extension diagram was drawn up by Instron and its data was extracted. The eggshell breaking force is determined by the force-deformation curve. So that in the shell breaking force, there is a large change in the force in the curve [16].

Figure 3. The egg quasi-static loading diagram (1) Force deformation machine; (2) the location of the egg

Figure 4. Schematic form of the egg physical characteristics for various forces

Principal component analysis

In this study, the collected data were analyzed using The Unscrambler X 10.4 (64-bit) software. Originally developed by Harald Martens and later enhanced by CAMO, this software is recognized as a specialized tool for multivariate data analysis. Its key features include data calibration, predictive modeling, and the implementation of advanced chemometric techniques. Principal component analysis was employed as one of the primary analytical methods to examine correlations among different variables, including broad-edge, thin-edge, and impact scores, as well as physical and chemical loadings. PCA transforms a set of correlated variables into a limited number of independent variables (principal components), allowing for dimensionality reduction and noise elimination. This method not only compresses data but also preserves the maximum variance, enabling a more accurate interpretation of the underlying data structure. As an unsupervised technique, PCA does not require the definition of a dependent variable, relying solely on intrinsic data relationships. This feature makes PCA particularly effective for exploratory studies and for identifying hidden patterns or natural groupings within datasets. Such analyses assist researchers in assessing inter-variable relationships with greater precision, ultimately leading to the development of more reliable and optimized models [17].

Results and Discussion

Principal component analysis

The collected data were analyzed using The Unscrambler X 10.4 (64-bit) chemometric software. The main strength of Unscrambler X lies in its ability to provide robust tools for the analysis of various types of multivariate data. It offers functionalities for data calibration and predictive modeling. Originally developed by Harald Martens and later enhanced by CAMO, the software supports principal component analysis, Partial least squares (PLS) regression, multivariate curve resolution, and other advanced analytical techniques. In this study, PCA was applied to examine the correlations between irradiation treatments, the number of lamps, and exposure time (scores) and the physical and chemical characteristics of the eggs (loadings). This method reduces a large set of interrelated variables into a smaller number of uncorrelated components while minimizing noise. Essentially, PCA serves as a data compression technique, transforming correlated variables into new, uncorrelated variables known as principal components. This process reduces the dimensionality of the feature space and is classified as an "unsupervised" method, meaning it does not require the definition of a dependent variable [17].

Ultraviolet radiation differences

Figure 5 presents PCA used to assess differences resulting from UV irradiation based on the physical and chemical properties of the samples. It consists of two sections: A (scores plot) and B (correlation loadings l\plot). In section A, known as the scores plot, the positioning of the samples is displayed according to the two principal components, PC1 and PC2. The first component (PC1) explains the largest portion of the variance, while the second component (PC2) accounts for the next highest level of variation. Each sample group is labeled according to the UV intensity applied—UV20, UV40, and UV60—represented by different symbols and colors. The UV40 data show greater dispersion along both principal components compared to UV20 and UV60, indicating more diverse changes in physical and chemical properties under these conditions. Conversely, the UV20 samples are mostly concentrated on the right-hand side and in the positive region of PC1, suggesting distinct compositional characteristics compared to other groups. UV60 samples, compared with UV40, are more densely clustered and tend to align toward the positive region of PC1, implying higher similarity in their attributes. The Hotelling's

T² ellipse illustrates the 95% confidence interval, with most points falling within the boundary, indicating an absence of significant outliers. Figure 5B shows the direction and strength of the correlation between each physical and chemical characteristic and the principal components. Each point represents a variable, and its position in the PC1–PC2 space indicates its contribution to explaining the variance in the dataset. For instance, Volume is located on the right side near the unit circle boundary, suggesting a strong correlation with PC1 and a key role in distinguishing between groups. Similarly, Crude protein and Sphericity are positioned in the positive PC1 region, though slightly inclined toward PC2, indicating partial association with both components. Crude fat also shows a positive correlation with PC1 but to a lesser extent than Volume. In contrast, Total Ash and Breaking Force are located in the negative regions of both PC1 and PC2, reflecting an opposite influence compared to variables such as Volume. Meanwhile, pH and Density are positioned near the center, indicating a relatively smaller contribution to overall variance compared to other traits. Comparing plots A and B reveals that the distribution of samples in the scores plot (A) directly corresponds to the positioning of physical and chemical variables in the correlation loadings plot (B). For instance, because Volume lies in the positive PC1 region, groups positioned there (e.g., most UV60 samples) likely exhibit higher Volume values. Conversely, groups in the negative PC1 region, such as UV20, are likely associated with higher Total Ash content or related attributes. Overall, the PCA effectively distinguishes between UV irradiation groups based on multiple quality parameters. The UV40 group exhibits the highest internal variability, possibly reflecting an optimal or more sensitive response at this irradiation level. Meanwhile, UV20 and UV60 display distinct patterns along the negative and positive PC1 regions, respectively, driven by variations in traits such as Volume, Crude Protein, and Total Ash. These findings provide valuable insights into the effects of UV intensity and support optimization of irradiation conditions to achieve desirable physicochemical properties in eggs.

Figure 5. Graph (Scores) from Principal Component Analysis (PCA) to separate the number of UV lamps based on physical and chemical properties

Infrared radiation differences

Figure 6. Graph (scores) from principal component analysis (PCA) for the number of IR lamp separations based on physical and chemical properties

Infrared and Ultraviolet radiation differences

According to Figure 6A, the first principal component (PC1) accounts for 100% of the variance, capturing all variations present in the dataset. This proportion indicates that the primary separation and differentiation of samples are entirely driven by PC1. In other words, most physical and chemical characteristics influenced by IR irradiation exhibit changes that are predominantly aligned along PC1. The scores plot illustrates the positioning of samples in the two-dimensional space defined by the principal components. IR20 samples are mainly located on the positive side of PC1, suggesting higher values for characteristics positively associated with this axis. The IR60 group is also concentrated in the positive PC1 region but displays tighter clustering, indicating greater similarity within this group and a stronger effect of high-intensity IR exposure. IR40 samples, however, are more dispersed between the two groups, showing the highest internal variability—some samples align closely with IR20, while others approach IR60. This pattern reflects a transitional or intermediate state of characteristics under moderate IR exposure. The loadings plot displays the relationship between physicochemical variables and

principal components. Volume shows the highest positive correlation with PC1, playing a significant role in differentiating the IR60 group. Crude protein and Sphericity also align with the positive PC1 region, contributing to the separation of samples exposed to higher IR levels. Conversely, Total Ash and Breaking Force are positioned in the negative PC1 or negative PC2 regions, placing them closer to the IR20 group. pH and Density appear near the center, indicating a smaller influence on overall group differentiation. Combining both plots demonstrates that IR intensity has a clear impact on the pattern of physicochemical characteristics. PC1 serves as the primary axis of separation, reflecting major variations such as increased volume and sphericity at higher irradiation levels (IR60) and increased total ash content at lower irradiation levels (IR20). IR40 occupies an intermediate position, with greater dispersion indicating a transitional stage in sample response to IR treatment. Overall, this PCA analysis not only reveals distinct group separations but also identifies the key variables responsible for these differences, enabling a deeper scientific interpretation of the relationship between IR intensity and structural—chemical changes in eggs.

In the PCA analysis, the contribution of each principal component to the total variance was first examined. Results indicated that PC1 alone accounted for the largest share of variance (100% of the significant variance). This finding suggests that the main differences among samples can be represented along a single dimension, with PC1 providing a highly accurate depiction of these variations. In Figure 7A, samples subjected to IR and UV treatments are clearly separated, forming two distinct clusters. The close proximity of points within each cluster indicates good repeatability and high similarity among samples within the same treatment group. Since the horizontal axis (PC1) explains nearly all variance, the observed separation is largely attributed to the variables represented by this component. Figure 7B shows that variables such as Volume, Density, and Breaking Resistance have the highest loadings on PC1, making them the most influential in differentiating between treatments. Most variables exhibit similar orientations and high correlations with one another, suggesting that they may change simultaneously under the influence of irradiation type. The PCA results revealed that the effects of IR and UV irradiation on the physicochemical properties of the samples are clearly distinct, with these differences being primarily explained by PC1. Physical attributes, such as volume and density, play the most significant roles in this separation, whereas chemical variables contribute to a lesser extent. These findings provide a valuable basis for focusing on key traits in future studies.

Figure 7. Scores from Principal Component Analysis (PCA) to separate the number of IR UV lamps - based on physical and chemical properties

Time Radiation Differences

The variance analysis of the components revealed that PC1 alone explained 100% of the total variance, while other components contributed negligibly. This result indicates that nearly all variations between IR-T1 and UV-T1 samples are concentrated along a single principal dimension, allowing for a precise interpretation of differences based solely on PC1. In Figure 8A, samples subjected to IR-T1 and UV-T1 treatments are clearly separated, forming two distinct clusters. UV-T1 samples (blue squares) are closely grouped, displaying a compact clustering pattern that suggests greater homogeneity in response to ultraviolet irradiation. In contrast, IR-T1 samples (red circles) exhibit greater dispersion, indicating higher variability in response to infrared exposure. The considerable distance between the centers of the two clusters highlights a fundamental difference between the effects of these two types of irradiation on sample properties. Figure 8B illustrates that most variables are concentrated within a specific

region and show strong intercorrelation. Volume, density, and breaking force exhibit the highest loadings on PC1, making them the key factors driving treatment separation. Other variables, such as Crude Fat, crude protein, starch, and total ash, are positioned further from the cluster center, reflecting a more moderate or treatment-specific influence. The similar orientation of all variables within the same half-plane indicates that their changes are aligned and likely occur simultaneously with variations in irradiation type. PCA results at T1 demonstrate that the effects of IR and UV irradiation on samples differ significantly, with these differences being almost entirely explained by PC1. The more compact clustering of UV-T1 indicates greater consistency and uniformity under UV treatment, while the wider spread of IR-T1 reflects a higher degree of variability in response to IR exposure. Physical variables such as volume, density, and breaking force play the primary roles in distinguishing the two treatments and may serve as key indicators for future studies.

In Figures 8C and 5D, principal component variance analysis revealed that PC1 alone accounted for 100% of the total variance, while the remaining components contributed negligibly. This indicates that nearly all differences between IR-T2 and UV-T2 samples are captured along a single principal dimension (PC1), enabling the interpretation to be primarily based on this component. In Figure 8C, IR-T2 and UV-T2 samples are clearly separated, forming two distinct clusters. IR-T2 samples (red circles) exhibit a more compact and closely grouped cluster, indicating greater uniformity in response to infrared irradiation. In contrast, UV-T2 samples (blue squares) display greater dispersion, suggesting higher variability in response to ultraviolet exposure. The considerable distance between the centers of the two clusters highlights a fundamental difference in the effects of these two irradiation types at stage T2. Figure 8D shows that most variables are concentrated within a specific region and display strong intercorrelation. Variables such as Volume, Density, Cooking Force, and Cooking Time have the highest loadings on PC1 and play a key role in distinguishing between the two treatments. Variables such as Crude Fat and Total Ash are positioned slightly further from the cluster center, indicating a more moderate or treatment-specific role. The similar orientation of all variables within the positive half-plane of PC1 suggests that their variations are aligned and likely influenced by similar irradiation effects. At stage T2, PCA results demonstrate that the effects of IR and UV irradiation on sample properties are substantially different, with these differences fully explained by PC1. Infrared irradiation induces a more uniform and consistent response, whereas ultraviolet irradiation results in greater variability among sample characteristics. Physical and functional attributes such as Volume, Density, and cooking parameters play a decisive role in this differentiation and can be considered key indicators for assessing irradiation effects at this stage. In Figures 8E and 5F, principal component variance analysis revealed that PC1 alone accounted for the entire variance in the dataset. This indicates that all observed differences between IR-T3 and UV-T3 samples are concentrated along a single principal dimension (PC1), making its analysis sufficient for interpreting the results. In Figure 8E, IR-T3 samples (red circles) are located in the upper-right region, while UV-T3 samples (blue squares) are positioned in the lower-left region, indicating a complete contrast in their PC1 and PC2 values. The IR-T3 cluster is more compact, reflecting a high level of uniformity in response to infrared irradiation, whereas the UV-T3 cluster shows greater dispersion, suggesting higher variability in response to ultraviolet exposure. The substantial distance between the centers of the two clusters highlights a fundamental difference in the sample properties. Figure 8F further illustrates that the Volume variable exhibits the highest positive loading on PC1, making it a key factor in distinguishing the IR-T3 group. Conversely, Total Ash displays the highest negative loading and is more closely

associated with the UV-T3 group. Other variables, including Crude Protein, Starch, Breaking Force, Density, and Crude Fat, are located near the center, suggesting moderate or combined contributions to group differentiation. This arrangement demonstrates the opposing effects of Volume and Total Ash in driving group separation. At stage T3, PCA results confirm that the difference between infrared and ultraviolet irradiation effects is strongly pronounced and fully explained by PC1. Infrared exposure induces a more uniform and concentrated response in sample attributes, whereas ultraviolet exposure results in greater variability. Volume was identified as the primary indicator for the IR-T3 group, while Total Ash served as the main distinguishing variable for the UV-T3 group, with other variables playing moderating or shared roles.

The greater variability observed under UV exposure may be due to its higher photon energy and surface-restricted penetration, which can trigger localized photochemical reactions, leading to heterogeneous responses among samples. In contrast, IR irradiation provides more uniform heating and deeper penetration, resulting in a more homogeneous response. This difference in interaction mechanisms between UV and IR likely underlies the variability pattern observed in PCA.

Figure 8. Graph (Scores) from Principal Component Analysis (PCA) for separating IR UV irradiation time - based on physical and chemical properties

Lamp Number Radiation Differences

Principal component analysis for the IR20 and UV20 treatments (Figures 9A and 6B) revealed that the first principal component (PC1) accounted for 100% of the total variance, indicating that all variability among samples is captured along a single dimension. Figure 9A clearly shows separation between IR20 and UV20 samples, with IR20 samples located on the positive side of the PC1 axis and UV20 samples clustered on the negative side. The high density of points within each group indicates strong homogeneity in their responses to irradiation, while the substantial distance between clusters highlights the pronounced effect of irradiation type on sample characteristics. Figure 9B demonstrates that Total Ash, Breaking Force, and Crude Protein show strong positive correlations with PC1 and play a key role in distinguishing IR20 samples. Conversely, Crude Fat, pH, and Volume exhibit negative correlations with PC1 and are more closely associated with the UV20 group. Density lies near the center, indicating a weaker contribution to group separation. These patterns suggest that key physical and chemical attributes are primarily responsible for the observed differences between irradiation types. For the IR40 and UV40 treatments, PCA analysis confirmed that PC1 again accounted for 100% of the total variance, with PC2 contributing negligibly to group differentiation. Figures 9C and 6D illustrate a clear and complete separation between IR40 and UV40 samples along the PC1 axis. IR40 samples are primarily located in the upper-right quadrant (positive PC1 and PC2 values), while UV40 samples are positioned in the lower-left quadrant (negative PC1 and PC2 values). The compact clustering within each treatment reflects a high degree of internal homogeneity. Variable loading patterns indicate that Crude Fat, Breaking Force, Total Ash, and Crude Protein have strong positive correlations with PC1, associating them closely with IR40 samples. In contrast, Volume is the only variable with a notable negative correlation, linking it to UV40 samples. Other variables, such as Density and Surface Area, contribute moderately or weakly to group differentiation. Overall, PCA for both IR20-UV20 and IR40-UV40 treatments confirms that irradiation type has a pronounced effect on sample characteristics, with physical and

chemical properties—particularly Crude Fat, Breaking Force, Total Ash, Crude Protein, and Volume—serving as the primary indicators for distinguishing between treatments.

Figure 9. Score plots from Principal Component Analysis (PCA) illustrating the separation of IR and UV lamp treatments based on physical and chemical properties

Conclusion

Principal component analysis was employed in this study to comprehensively investigate the effects of UV and IR irradiation on the physical and chemical properties of the samples. Results indicated that the first principal component (PC1) accounted for the largest proportion of the variance in all analyses and, in some cases, explained 100% of the total variation. This demonstrates that the differences among samples were largely concentrated in a single principal dimension, primarily influenced by irradiation type and its impact on key attributes such as volume, density, breaking strength, total ash, crude protein, and crude fat. For UV treatments, samples exposed to UV20 and UV60 exhibited distinct patterns along the positive and negative axes of PC1, whereas UV40 showed greater dispersion, indicating higher variability in response at this irradiation level. In contrast, IR irradiation produced more compact and homogeneous clusters, particularly in IR60 and IR-T3 treatments, reflecting a more uniform response to infrared exposure. Comparative analysis of UV and IR treatments revealed fundamentally different effects on sample characteristics. Overall, UV irradiation induced greater variability in both physical and chemical properties, while IR irradiation resulted in more consistent responses. Physical parameters such as volume and density played key roles in discriminating among treatments, while chemical variables like crude protein and total ash also contributed significantly in certain cases. Moreover, the results demonstrated that increasing irradiation time (T1 to T3) intensified the differences between treatments, with variables more distinctly separating the groups. In summary, this study highlights that the type and intensity of irradiation (UV or IR) exert distinct influences on sample characteristics. PCA proved to be a powerful tool for identifying key variables and effectively differentiating treatment groups based on physicochemical properties. These findings provide a foundation for future research aimed at optimizing irradiation conditions to achieve desirable product characteristics. Furthermore, identifying influential variables such as volume and total ash may facilitate the development of rapid and accurate quality assessment methods under various irradiation conditions. Ultimately, integrating multivariate analyses like PCA with experimental studies offers deeper insight into the effects of environmental factors on material properties.

Conflict of interest

No conflict of interest has been declared by the authors

References

- [1] Eddin, A. S., Ibrahim, S. A., & Tahergorabi, R. (2019). Egg quality and safety with an overview of edible coating application for egg preservation. Food chemistry, 296, 29-39. https://doi.org/10.1016/j.foodchem.2019.05.182.
- [2] Stadelman, W. J. (2017). Quality identification of shell eggs. In Egg science and technology. CRC Press. 39-66.
- [3] Soliman, A., & Safwat, A. M. (2020). Climate change impact on immune status and productivity of poultry as well as the quality of meat and egg products. In Climate change impacts on agriculture and food security in Egypt: Land and water resources Smart farming

- livestock, fishery, and aquaculture. Cham: Springer International Publishing. 481-498. https://doi.org/10.1007/978-3-030-41629-4_20.
- [4] Luo, W., Xue, H., Xiong, C., Li, J., Tu, Y., & Zhao, Y. (2020). Effects of temperature on quality of preserved eggs during storage. Poultry science, 99(6), 3144-3157. https://doi.org/10.1016/j.psj.2020.01.020.
- [5] Feddern, V., Prá, M. C. D., Mores, R., Nicoloso, R. D. S., Coldebella, A., & Abreu, P. G. D. (2017). Egg quality assessment at different storage conditions, seasons and laying hen strains. Ciência e Agrotecnologia, 41(3), 322-333. https://doi.org/10.1590/1413-70542017413002317.
- [6] Yimenu, S. M., Kim, J. Y., & Kim, B. S. (2017). Prediction of egg freshness during storage using electronic nose. Poultry science, 96(10), 3733-3746. https://doi.org/10.3382/ps/pex193.
- [7] Qi, L., Zhao, M. C., Li, Z., Shen, D. H., & Lu, J. (2020). Non-destructive testing technology for raw eggs freshness: A review. SN Applied Sciences, 2(6), 1113. https://doi.org/10.1007/s42452-020-2906-x.
- [8] Gholizadeh, S. (2016). A review of non-destructive testing methods of composite materials. Procedia structural integrity, 1, 50-57. https://doi.org/10.1016/j.prostr.2016.02.008.
- [9] Wang, Q., Yang, Z., Liu, C., Sun, R., & Yue, S. (2025). Research Progress on Non-Destructive Testing Technology and Equipment for Poultry Eggshell Quality. Foods, 14(13), 2223. https://doi.org/10.3390/foods14132223.
- [10] Sehirli, E., & Arslan, K. (2022). An application for the classification of egg quality and haugh unit based on characteristic egg features using machine learning models. Expert Systems with Applications, 205, 117692. https://doi.org/10.1016/j.eswa.2022.117692.
- [11] Cedro, T. M. M., Calixto, L. F. L., Gaspar, A., Curvello, F. A., & Hora, A. S. (2009). Internal quality of conventional and omega-3-enriched commercial eggs stored under different temperatures. Brazilian Journal of Poultry Science, 11, 181-185. https://doi.org/10.1590/S1516-635X2009000300007.
- [12] Moore, B. (2003). Principal component analysis in linear systems: Controllability, observability, and model reduction. IEEE transactions on automatic control, 26(1), 17-32.
- [13] Azadbakht, M., Torshizi, M. V., Ziaratban, A., & Ghajarjazi, E. (2016). Application of Artificial Neural Network (ANN) in predicting mechanical properties of canola stem under shear loading. Agricultural Engineering International: CIGR Journal, 18(2), 413-425.
- [14] Mahmoodi, M. J. M., Azadbakht, M., Asghari, A., & Dastar, B. (2020). Evaluation of the effect of UV light on the biochemical properties of egg internal contents using the response surface method. Innovative Food Technologies, 7(3), 365-378. https://doi.org/10.22104/jift.2020.3560.1856.
- [15] Mahmoodi, M. J., Azadbakht, M., Asghari, A., & Dastar, B. (2022). Ultraviolet and infrared rays effects on some mechanical properties of oil-stained eggshells using response surface methods. Iran Agricultural Research. 40(1), 9-15. https://doi.org/10.22099/IAR.2021.39441.1425.
- [16] Mahmoodi, M. J., Azadbakht, M., Asghari, A., & Dastar, B. (2019). Investigating the amount of resistance to break the eggshell under the influence of a strong magnetic field (MRI). Poultry Science Journal. 7(2), 101-108. https://doi.org/10.22069/psj.2019.16316.1412.
- [17] Kamboj, U., Kaushal, N., & Jabeen, S. (2020, May). Near Infrared Spectroscopy as an efficient tool for the Qualitative and Quantitative Determination of Sugar Adulteration in Milk. In Journal of Physics: Conference Series. 1531(1), 012024. https://doi.org/10.1088/1742-6596/1531/1/012024.

Figures:

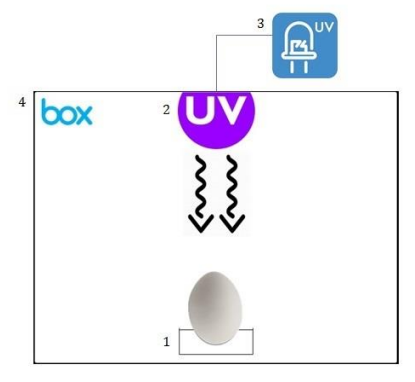


Figure 1. Schematic of the circuit and the UV radiation method (1) Sample location; (2) lamp circuit; (3) radiation chamber

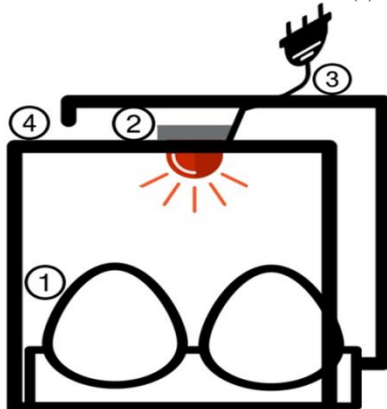


Figure 2. Schematic of the circuit and the IR radiation method (1) Sample location; (2) lamp circuit; (3) radiation chamber

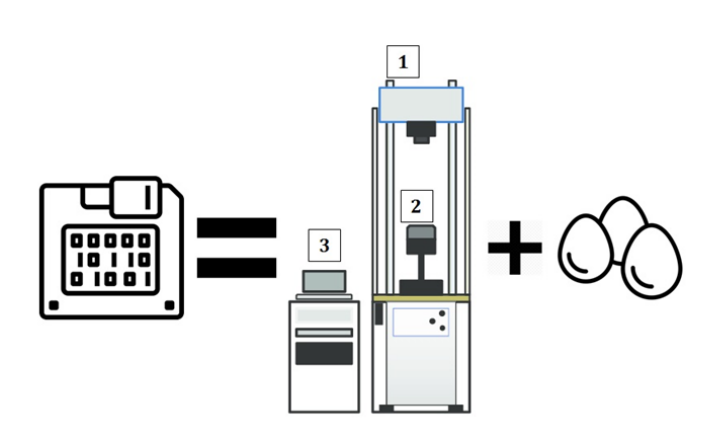




Figure 3. The egg quasi-static loading diagram (1) Force deformation machine; (2) the location of the egg

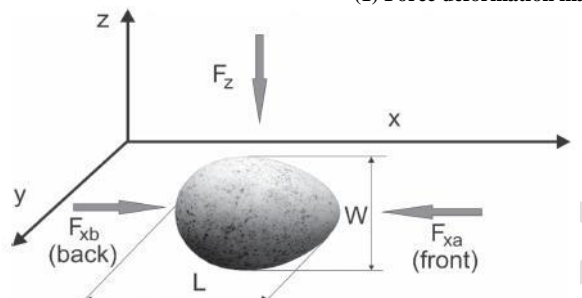


Figure 4. Schematic form of the egg physical characteristics for various forces

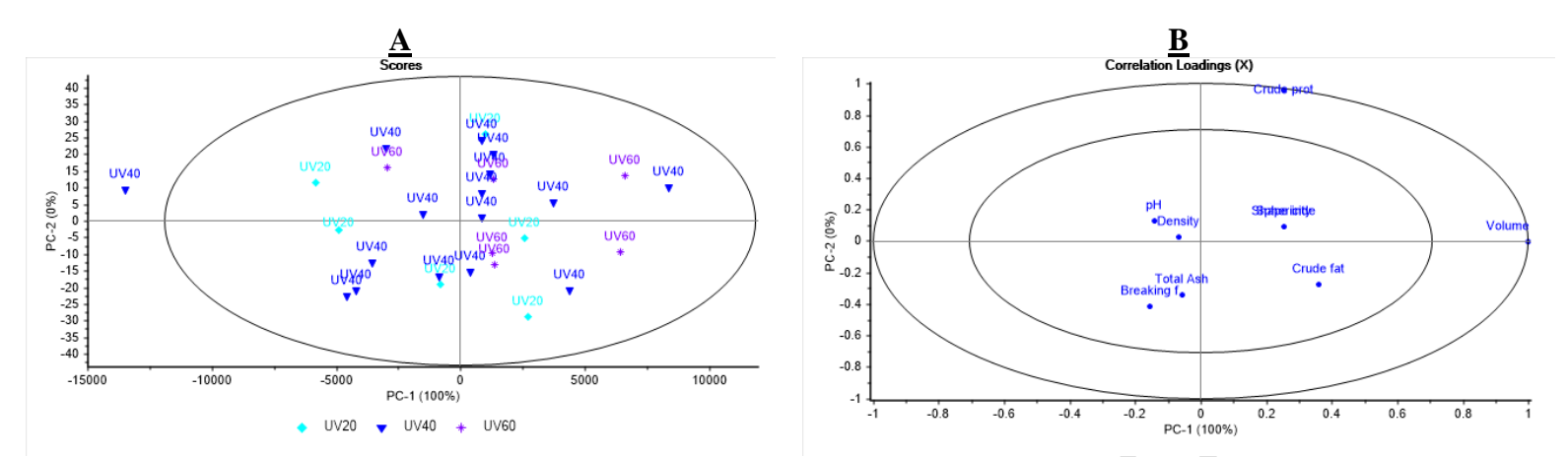


Figure 5. Principal component analysis score plot for the separation of samples based on the number of ultraviolet lamp treatments and their effects on physical and chemical properties.

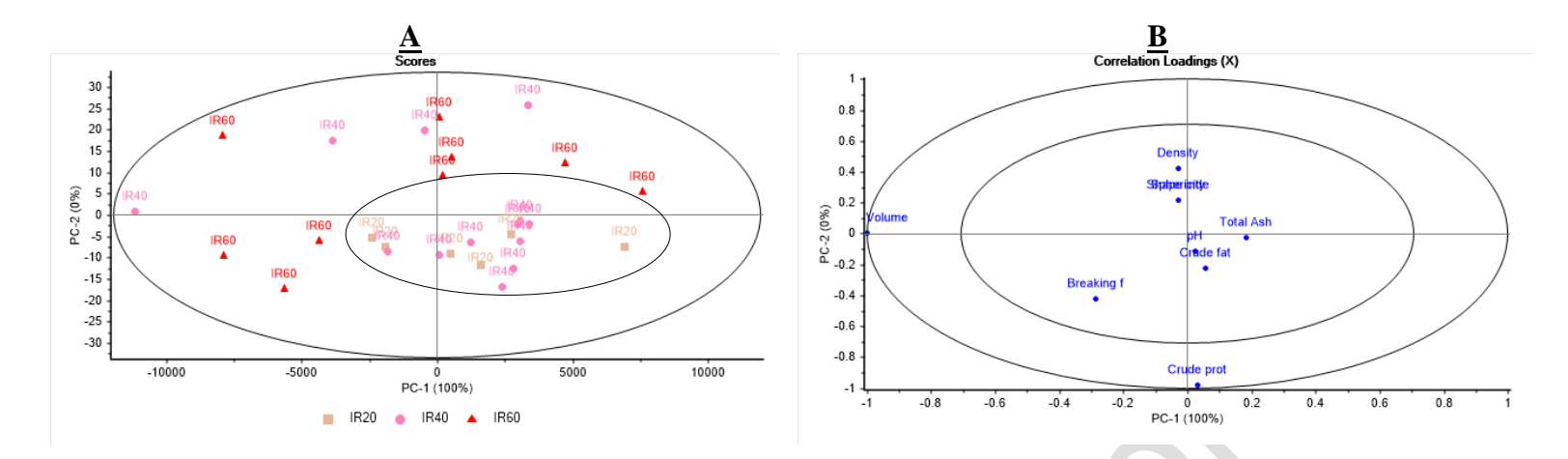


Figure 6. Principal component analysis score plot for the separation of samples based on the number of infrared lamp treatments and their effects on physical and chemical properties.

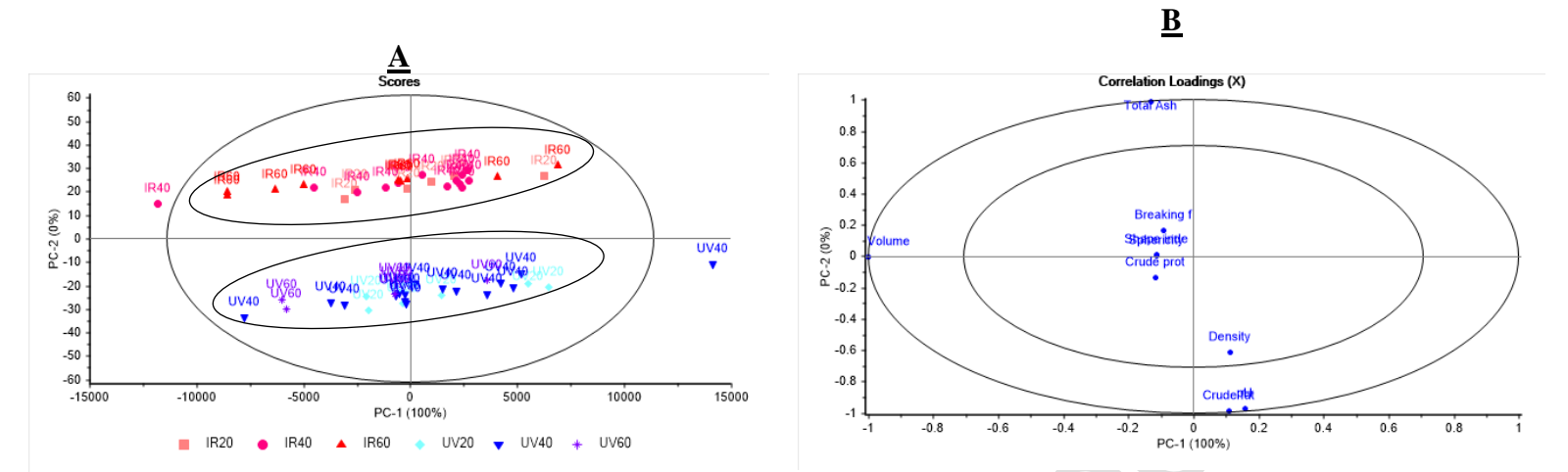


Figure 7. Principal component analysis score plot comparing the effects of infrared and ultraviolet lamp treatments on physical and chemical properties.

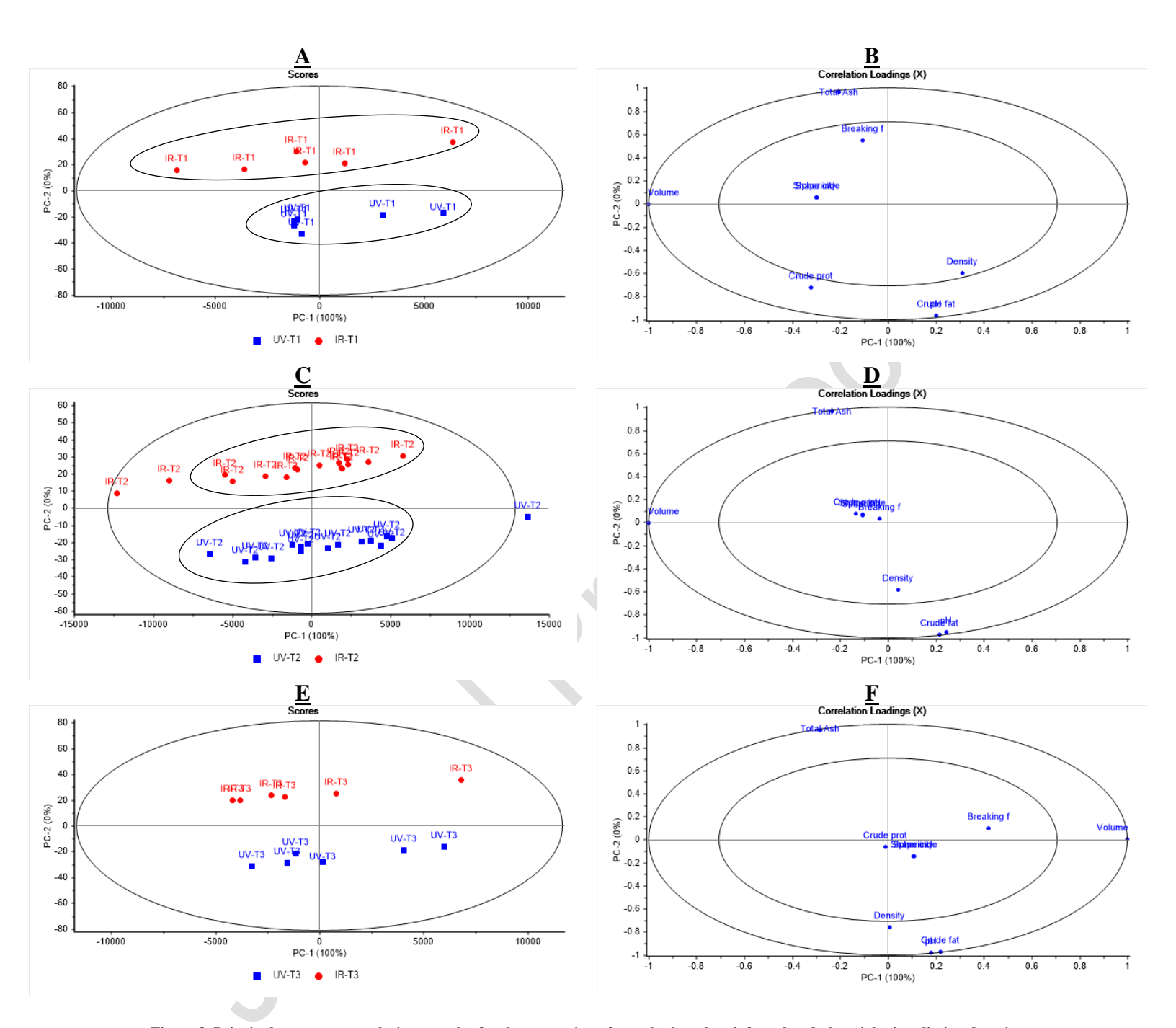


Figure 8. Principal component analysis score plot for the separation of samples based on infrared and ultraviolet irradiation duration and their effects on physical and chemical properties.

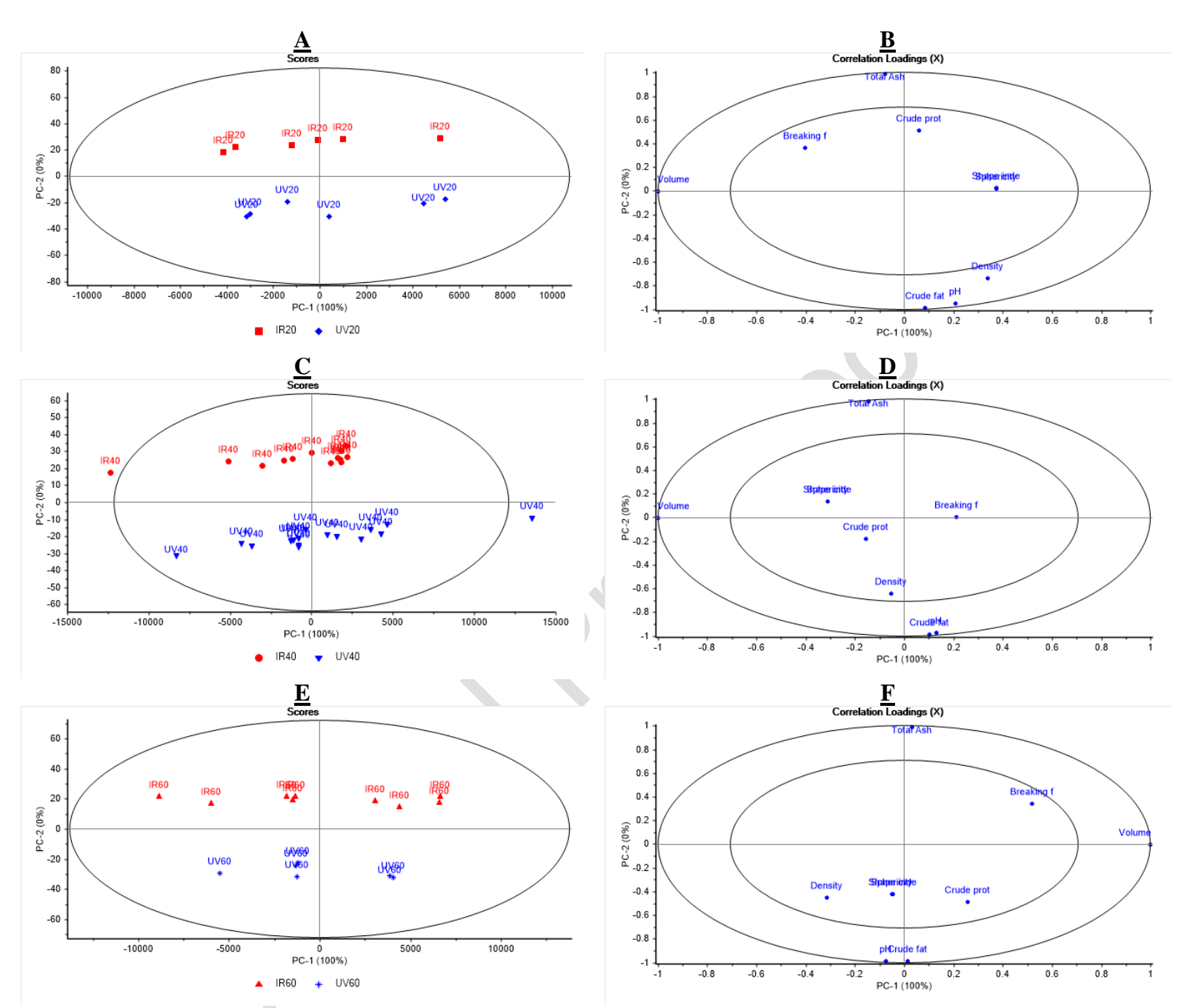


Figure 9. Principal component analysis score plots illustrating the separation of samples subjected to different infrared and ultraviolet lamp treatments based on physical and chemical properties.